ELSEVIER

Thermochimica Acta 278 (1996) 135–144

thermochimica acta

Structure and thermal decomposition of lithium-manganese dicarboxylate systems

Tomoki Tsumura [a], Satoru Kishi [b], Hidetaka Konno [a], Akira Shimizu [a], Michio Inagaki [a,*]

[a] *Faculty of Engineering, Hokkaido University, Kita-Ku, Sapporo 060, Japan*

[b] *Rigaku Corporation, Nishishinjyuku, Shinjyuku-Ku, Tokyo 160, Japan*

Received 1 June 1995; accepted 23 September 1995

Abstract

Lithium-manganese dicarboxylates were prepared as a precursor for the synthesis of $LiMn_2O_4$ spinel. The structure and thermal decomposition of dicarboxylates were investigated by means of DTA–TG–MAS, XRD, and FTIR measurements. The results indicated that malonate and tartrate form a mixture of lithium-manganese complex salt and manganese salt, but oxalate and succinate have a chain-like structure in which lithium and manganese ions are linked by a dicarboxylic acid ion. For all dicarboxylates, there is no growth of crystalline intermediates during their decomposition process. Beacuse of its low decomposition temperature, 260°C, the malonate was the most suitable precursor for the preparation of $LiMn_2O_4$ spinel.

Keywords: Dicarboxylate; $LiMn_2O_4$ spinel; Precursor

1. Introduction

In recent years, interest in Li rechargeable batteries has greatly increased worldwide [1,2]. $LiMn_2O_4$, which has a spinel structure, is one of the candidates for the cathode of high-energy-density Li batteries [3–5]. $LiMn_2O_4$ powders are mainly prepared by reacting a mixture of Li_2CO_3 and MnO_2 powders in air above 600°C, followed by several successive grinding and annealing sequences. The chemical reactivity of the powders is known to be strongly influenced by surface area and particle morphology, this being the case in the cathodic performance of $LiMn_2O_4$ powders as well. The

* Corresponding author.

SSDI 0040-6031(95)02759-9

stochiometry and also the cation distribution in $LiMn_2O_4$ spinel have been pointed out as being important factors to be controlled for cathode materials [6]. In the solid state reaction between Li_2CO_3 and MnO_2, however, it is difficult to control these factors, because some lithium oxides evaporate from the reaction system, which deteriorates the stoichiometry of the resulting compounds, and also accelerates the grain growth of the crystal, which results in heterogeneity of particle size. Therefore, it is important to develop a new process for the synthesis of $LiMn_2O_4$ powders which can proceed at low temperatures. We proposed a simple route, i.e., synthesis of $LiMn_2O_4$ powders via lithium-manganese tartrates [7]. Using this method, $LiMn_2O_4$ powders were prepared above 250°C, in which the particle size was uniform and below 0.1 μm. Starting from the powders thus prepared at low temperatures, it was possible to study the effect of the crystallinity of $LiMn_2O_4$ on cathodic performance in lithium secondary cells [8].

In the present work, the thermal decomposition of lithium-manganese dicarboxylates to the $LiMn_2O_4$ spinel investigated to determine the effects of dicarboxylic acid ions. Four dicarboxylates, oxalate, malonate, succinate and tartrate, were selected. From the experimental results obtained, we propose two types of structure for these dicarboxylates; a mixture of lithium-manganese complex and manganese salts (malonate and tartrate systems) and a chain-like structure in which lithium and manganese ions are linked by dicarboxylic acid ion (oxalate and succinate systems). Because of its lowest decomposition temperature of 260°C, the malonate was proposed as the most suitable precursor for the synthesis of $LiMn_2O_4$ powders.

2. Experimental

2.1 Preparation

The procedure for the preparation of $LiMn_2O_4$ spinel powder from lithium and manganese acetates through lithium-manganese dicarboxylates is shown schematically in Fig. 1. Oxalic acid ($C_2H_2O_4$), malonic acid ($C_3H_4O_4$) and succinic acid differ only in the number of carbon atoms, but tartaric acid ($C_4H_6O_6$) has two hydroxyl groups with the same carbon number as succinic acid. Lithium acetate dihydrate and manganese acetate tetrahydrate (reagent grades) were dissolved in ethanol, the molar ratio of Li^+ to Mn^{2+} being 1 to 2. As soon as the solution was mixed with a dicarboxylic acid, the solution changed into a viscous sol. The molar concentration of dicarboxylic acid was the same as the total concentration of metal ions, i.e., lithium plus manganese ions. By heating the sol at 50°C, acetic acid and ethanol were evaporated, and a dry powder of lithium-manganese dicarboxylate was obtained. For comparison, lithium and manganese dicarboxylates were prepared separately by the same procedure, using a molar ratio between metal ion and dicarboxylic acid ion of 1 to 1.

2.2. XRD and FTIR measurements

The measurements of XRD powder patterns were performed on dicarboxylates and those heated at different temperatures, using Ni-filtered Cu Kα radiation with a scanning speed of 2° min^{-1}.

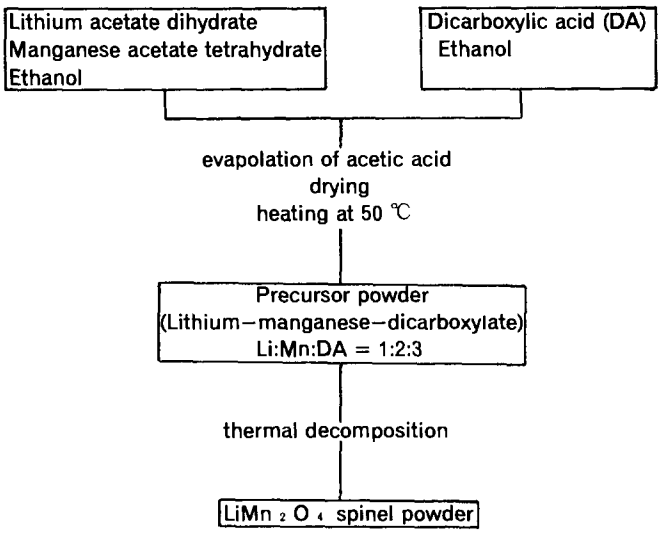

Fig. 1. Flowchart for the preparation of lithium-manganese dicarboxylates.

FTIR diffuse reflectance spectra were measured on the dicarboxylates which were mixed and diluted about 100 times with KBr powder.

2.3. *Thermal analysis*

The gases evolved during decomposition of the dicarboxylates were investigated by a mass analyzer coupled with a DTA–TG apparatus under He gas flow. The heating rate was 25 K min^{-1} up to 600°C. The product of this analysis was found by XRD to be a mixture of MnO and Mn_2O_3, an no lithium compound was detected.

DTA–TG analysis on the dicarboxylates was performed under static air with a constant heating rate of 1 K min^{-1}. There was no X-ray diffraction line, with the exception of $LiMn_2O_4$ spinel phase, in the products of the thermal analysis up to 600°C. The intermediates from dicarboxylates to spinel were sampled by quenching from different temperatures during the course of the thermal analysis and also characterized by XRD and FTIR at room temperature.

3. Results

3.1. *Tartrate system*

Structure

The XRD pattern of lithium-manganese tartrate (LMT), or the precursor, is shown in Fig. 2, where lithium tartrate (LT) and manganese tartrate (MT) are also presented.

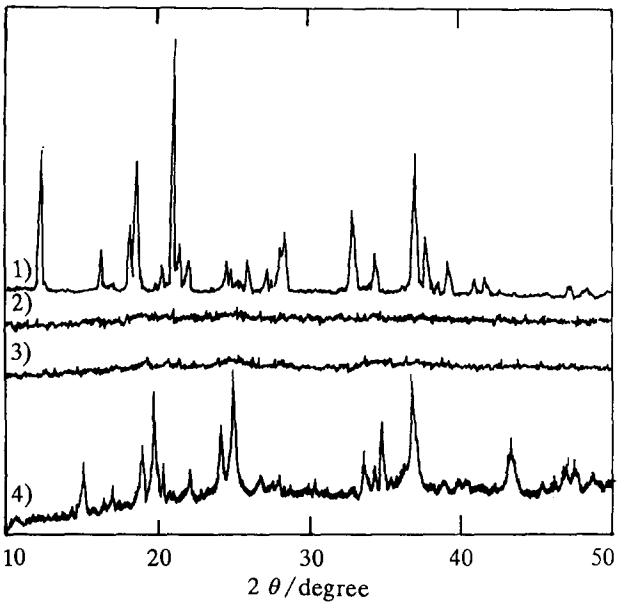

Fig. 2. XRD patterns of tartrates: 1, lithium tartrate (LT); 2, manganese tartrate (MT); 3, lithium-manganese tartrate (LMT); 4, LMT heated at 100°C for 24 h in static air with constant heating rate 1 K min^{-1}.

LT has a crystalline structure whose diffraction pattern resembles with that of tartaric acid itself [9], but MT and LMT are in an amorphous state. After heating at 100°C for 24 h in static air with a constant heating rate of 1 K min^{-1}, the sample LMT crystallized but its diffraction pattern could not be assigned to LT or MT.

The FTIR spectra of the tartrates are shown in Fig. 3a. In the spectrum of LMT, there are no absorption peaks which are attributable to LT. It is rather similar to that of MT. This implies that, in the structure of LMT, lithium ions are not bound by tartaric acid carboxyl group ions.

The result of DTA–TG–MAS analysis on LMT in He gas shown in Fig. 4a reveals weight losses in five steps, around 80, 160, 250, 320 and 380°C. The first step corresponds to the evolution of coordination water and the weight loss indicated that the molar ratio of H_2O to Mn^{2+} was 1 in the precursor. The decomposition of the alkyl chain of the tartaric acid ion occurs at the second, third and fourth steps with evolution of CH_2OH, C_2H_5OH and H_2O. The carboxyl group decomposes from the third to fifth steps with evolution of CO and CO_2. Since combustion of the organic component does not occur, all gas evolution takes place in parallel to the endothermic peak on the DTA curve. This reveals that both the alkyl chain and the carboxyl group of tartaric acid ion decompose in three different steps. Therefore, LMT is thought to have three tartaric acid ions with different thermal stabilities.

From the experimental results, we propose that the precursor, LMT, has the structure depicted in Fig. 5a; manganese ion is coordinated by two tartaric acid ions as bidentate to form a complex anion. the charge balance in LMT is achieved by the

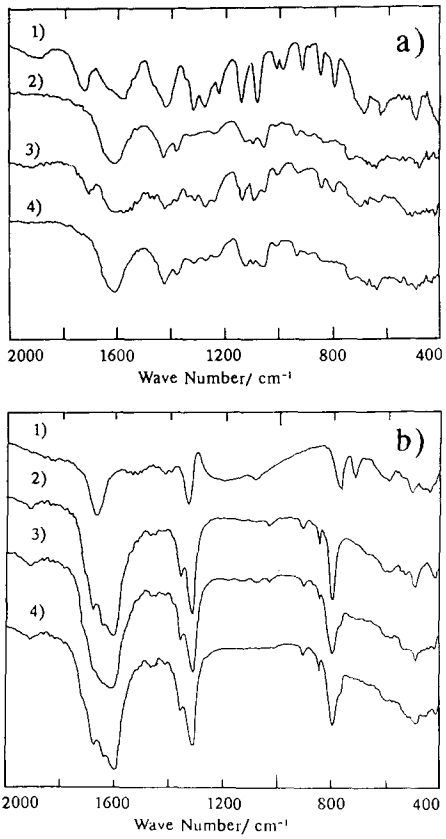

Fig. 3. FTIR spectra of tartrates (a) and oxalates (b): a-1, lithium tartrate (LT); a-2, manganese tartrate (MT); a-3, mixtures of LT and MT, the molar ratio of these salts being 1 to 2; a-4, lithium-manganese tartrate (LMT); b-1, lithium-oxalate (LO); b-2, manganese oxalate (MO); b-3, mixtures of LO and MO, the molar ratios of these salts being 1 to 2; b-4, lithium-manganese oxalate (LMO).

cations Li^+ and H^+. The crystalline phase which appeared by heating LMT at 100°C is attributed to the complex salt. The remaining manganese ions and tartaric acid ions bond with each other to form manganese tartrate.

Thermal decomposition

The DTA–TG curves for LMT in static air are presented in Fig. 6a. The decomposition takes place with combustion of the organic component. The TG curve for LMT shows that the weight loss occurs in three steps around 180, 250 and 290°C, all of them being accompanied by exothermic peaks on the DTA curve. The XRD pattern of the sample recovered at point A did not show diffraction lines and its FTIR spectrum was identical with that of the starting material, LMT. The sample recovered from point B did not reveal XRD lines either and, in its FTIR spectrum, the absorption peak of

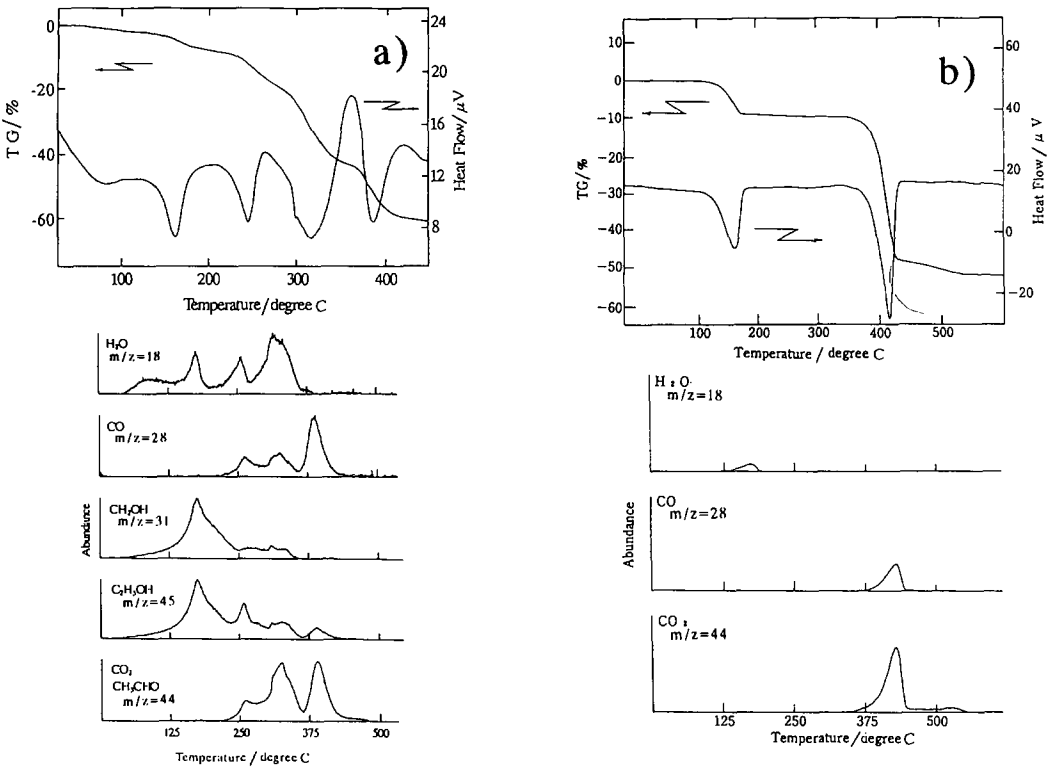

Fig. 4. DTA–TG curves and gaseous product in He gas: a, lithium-manganese tartrates (LMT); b, lithium-manganese oxalate (LMO).

Mn–O and Li–O bonds (300–800 cm^{-1}) [10] and the trace of the absorption peaks of CO_3^{2-} (800 cm^{-1} and 1400–1600 cm^{-1}) [11] and of tartaric acid ion (1300–1800 cm^{-1}) were observed. This indicated that crystalline intermediates were not formed during decomposition of the precursor LMT.

3.2. *Malonate system*

The precursor from the lithium-manganese malonate system (LMM) gave similar results for XRD, FTIR and DTA–TG analyses as LMT and, therefore, it seemed to consist of lithium-manganese malonate complex salt and manganese malonate.

3.3. *Oxalate system*

Structure

The XRD patterns of the oxalates were also similar to those of the tartrates. Lithium oxalate (LO) had a crystalline structure which resembled oxalic acid, but manganese

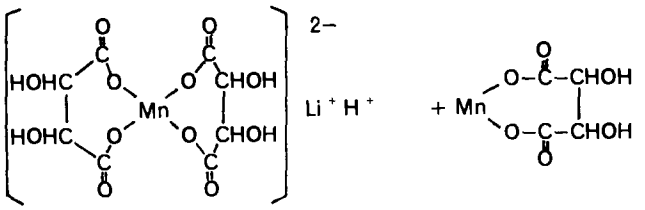

a)

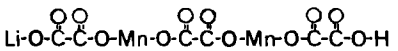

b)

Fig. 5. Proposed structure of lithium-manganese dicarboxylates: a, lithium-manganese tartrate (LMT); b, lithium-manganese oxalate (LMO).

oxalate (MO) and lithium-manganese oxalate (LMO), or the precursor, were in an amorphous state. However, the pattern of LMO heated at 100°C for 24 h in static air with constant heating rate, 1 K min^{-1}, showed several broad peaks. If it were a simple mechanical mixture of LO and MO, LO would crystallize by heating at 100°C. Thus it is concluded that this is not a simple mixture of these salts but that it has a structure which does not crystallize easily.

The FTIR spectra of the oxalates are shown in Fig. 3b. In the spectrum of LMO, an absorption peak at around 770 cm^{-1} and a peak shoulder at around 1740 cm^{-1}, which are attributed to LO are detected in addition to the peaks for MO, and the spectrum is similar to that of the mechanical mixture of LO and MO, the molar ratio of these salts being 1 to 2. In the structure of LMO, therefore, each manganese and lithium ion is thought to combine with the carboxyl group of the oxalic acid ions.

The result of DTA–TG–MAS analysis for LMO in He gas is shown in Fig. 4b. Three weight losses occur around 150, 400 and 500°C on the TG curve, and the first and second ones proceed with endothermic peaks on the DTA curve. The first weight loss is caused by evolution of H_2O, which is believed to be coordination water. This indicated that the number of water molecules is equal to that of the manganese ions in the precursor. The large second weight loss and small third one correspond to CO and CO_2 gas evolution due to the decomposition of oxalic acid ions. The result indicates that oxalic acid ions in LMO decomposed in one step, with no intermediate formed during its decomposition. Because the decomposition temperatures of LO and MO should be different, LMO was not a mixture of LO and MO. This suggests that every oxalic acid ion is attached to manganese ions in LMO.

From these results, a structure of LMO is proposed, as shown in Fig. 5b; lithium and manganese ions are linked by oxalic acid ions to form a chain-like structure.

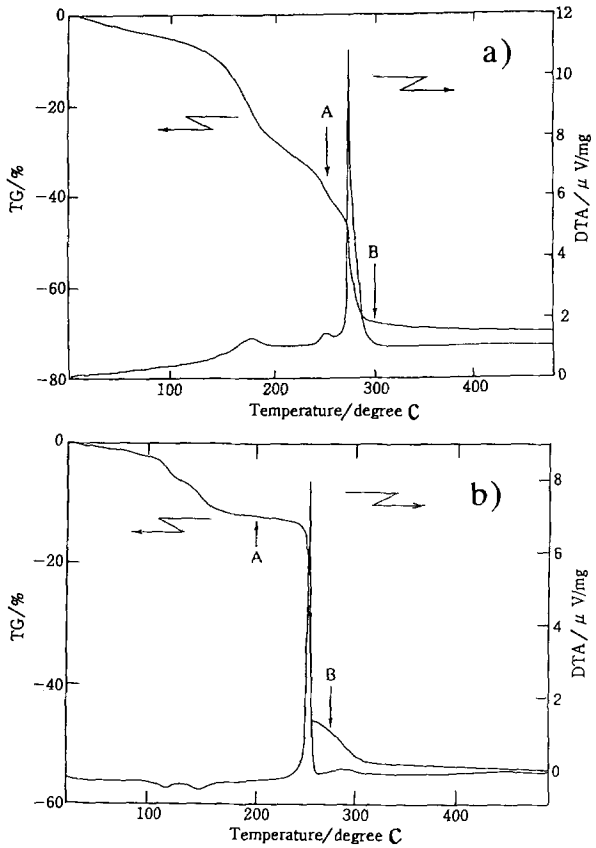

Fig. 6. DTA–TG curves in static air: a, lithium-manganese tartrate (LMT); b, lithium-manganese oxalate (LMO).

Thermal decomposition

The DTA–TG curves for LMO in static air are shown in Fig. 6b. The TG curve for LMO in static air are shown in Fig. 6b. The TG curve for LMO shows weight losses in four steps, around 110, 140, 260 and 290°C. Corresponding to these weight losses, two endothermic peaks are observed at the first and second steps, and sharp and broad exothermic peaks at the third and fourth steps, respectively. The XRD pattern of the sample at point A in the figure showed several broad peaks which were a little sharper than the peaks observed in the starting material, LMO. Its FTIR spectrum was identical with that of the starting material, LMO. The XRD pattern of the sample at point B showed no peaks. In this FTIR spectrum, Mn–O and Li–O bonds, CO_3^{2-} and oxalic acid ion (1300 and 1700 cm^{-1}) [12] were detected. A crystalline intermediate was not detected during the decomposition process.

3.4. Succinate system

Since lithium-manganese succinate (LMS) revealed similar results as LMO, the structure of LMS is also proposed to be a chain-like structure.

4. Discussion

4.1. Structure of lithium-manganese dicarboxylates

The experimental results indicate that the four lithium-manganese dicarboxylate systems are classified into two groups from their structures: tartrate and malonate forming a mixture of the complex salt, in which two carboxylic acid ions are bound to manganese ion in bidentate state, and manganese salt; and oxalate and succinate having a chain-like structure.

The size of the ring which will be made if the dicarboxylic acid ion coordinates to manganese ion as bidentate may be related to the structure that the dicarboxylate has. The increasing order of size is: oxalic acid < malonic acid, tartaric acid < succinic acid.

Oxalic acid ions seemed to have difficulties making a ring with the metal ion because of the strain energy to form a small ring, while the succinic acid ion was so large that it could not make a ring either because of the strain energy. Malonic and tartaric acids ions may be a suitable size to coordinate to manganese ion as bidentate, being free from strain energy. The geometrical issue might govern which structure type is taken by dicarboxylates.

4.2. Suitable precursor for $LiMn_2O_4$

As mentioned above, the lithium extraction/insertion reaction from $LiMn_2O_4$ in nonaqueous secondary lithium cells is influenced by its stoichiometry and particle size. Since $LiMn_2O_4$ spinel powders were prepared above 300°C using the present method via dicarboxylates, the loss of the lithium component during heat treatment is thought to be slight and, therefore, the stoichiometry can be controlled at the stage of the precursor preparation. The particle size of $LiMn_2O_4$ powders prepared were below 0.1 μm under SEM observation, larger particle sizes being easily obtained by high-temperature annealing.

Avoiding the formation of crystalline intermediate phase during decomposition is an additional advantage for the present process via dicarboxylates, because of the high possibility of obtaining powders with homogeneity in particle size, composition and structure.

In particular, of the four dicarboxylates investigated, the malonate may be the most suitable precursor for $LiMn_2O_4$ spinel because it has the lowest decomposition temperature in air at the heating rate 1 K min^{-1}, namely 260°C.

References

[1] Z. Takehara and K. Kanamura, Electrochim. Acta, 38 (1993) 1169.
[2] K.M. Abraham, Electrochim. Acta, 38 (1993) 1233.

[3] D. Guyomard and J.M. Tarascon, J. Electrochem. Soc., 140 (1993) 3071.
[4] T. Ohzuku, M. Kitagawa and T. Hirai, J. Electrochem. Soc., 137 (1990) 769.
[5] J.M. Tarascon, E. Wang, F.K. Shokoohi, W.R. McKinnon and S. Colson, J. Electrochem. Soc., 138 (1991) 2859.
[6] J.M. Tarascon, W.R. McKinnon, F. Coowar, T.N. Bowmer, G. Amatucci and D. Guyomard, J. Electrochem. Soc., 141 (1994) 1421.
[7] T. Tsumura, A. Shimizu and M. Inagaki, J. Mater. Chem., (1993), 3, 995.
[8] T. Tsumura, A. Shimizu and M. Inagaki, Solid State Ionics, to be submitted.
[9] ASTM diffraction file 40–610.
[10] P. Tarte and J. Preudhomme, Spectrochim. Acta, 29A (1972). 1301.
[11] M. Stockenhuber, H. Mayer and J.A. Lercher, J. Am. Ceram. Soc., 76 (1993) 1185.
[12] M.J. Schmerz, T. Miyazawa, S. Mizushima, T.J. Lane and J.V. Quagliano, Spectrochim. Acta, 9 (1957) 51.